A Uniform Asymptotic Analysis for Transient Scattered Fields by a Cylindrically Curved Open Surface with Varying Radius of Curvature

#Keiji Goto, Toshihide Ajiki, Toru Kawano, and Toyohiko Ishihara
Department of Communication Engineering, National Defense Academy
Hashirimizu, Yokosuka, 239-8686 Japan
E-mail: keigoto@nda.ac.jp

Abstract

The time-domain uniform asymptotic solution (TD-UAS) for the transient scattered field excited by the high-frequency (HF) pulse wave incident on a cylindrically curved open surface with a varying radius of curvature is presented in this paper. The TD-UAS, effective in the transition regions including the geometrical boundaries RB and SB, is constructed by the geometrical rays, the surface diffracted rays, the lowest order adiabatic whispering gallery mode radiation fields, and the combination of these pulse waves. The TD-UAS has an advantage that the total solution can be obtained from the summation of the individual solution which can easily be interpreted physically. We have confirmed the accuracy and the validity of the TD-UAS by comparing with the reference solution calculated from the combination of the method of moment (MoM) and the fast Fourier transform (FFT) code and with the reference solution obtained from the combination of the frequency-domain UAS and the FFT code.

1. INTRODUCTION

Recently, by the technological advances in high-resolution radar and electromagnetic pulses (EMP), it has become important to study the transient electromagnetic field radiated by an antenna or the transient scattered field produced by various objects [1], [2]. In the high-frequency (HF) analysis of the scattered field by an object with a complex shape, it is necessary to study the analysis method by an object with a relatively simple shape or the analysis method for the canonical problem [3]-[5].

The purpose of this paper is to derive the time-domain uniform asymptotic solution (TD-UAS) for the transient scattered field when the HF pulse wave is incident on a cylindrically curved open conducting surface with a varying radius of curvature. The accuracy and the validity of the TD-UAS proposed here are confirmed by comparing with the reference solutions calculated numerically from the combination of the frequency-domain (FD) numerical solution obtained from the method of moment (MoM) [6], [7] and the fast Fourier transform (FFT) code and from the combination of the frequency-domain uniform asymptotic solution (FD-UAS) [8] and the FFT code.

2. FORMULATION

Fig.1 shows the cylindrically curved open conducting surface Ω with varying radius of curvature, the curved coordinate system (s, q), the rectangular coordinate system (x, y, z), and the coordinate system (R, ψ). The origin of coordinate system (x, y, z) is chosen to coincide with the vertex point O of the curved surface Ω. Note that s and q in the coordinate system (s, q) are the distance along the curved surface measured from the point O and the vertical distance from the curved surface, respectively.

We assume that the radius of curvature $a(s)$ is sufficiently larger than the wavelength $\lambda\,(=2\pi c/\omega)$ (ω and c are the

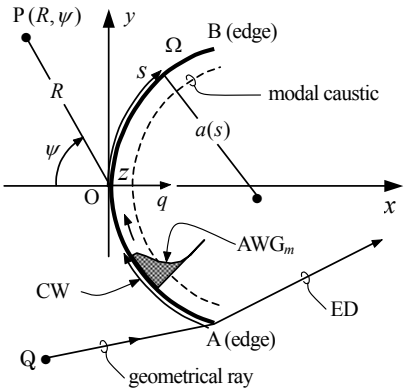

Fig.1 Cylindrically curved open conducting surface Ω with varying radius of curvature, coordinate systems (x, y, z), (s, q), and (R, ψ). A, B: straight edges, Q: magnetic line source, P: observation point. Also shown are edge diffracted ray (ED), creeping wave (CW), and mth order adiabatic WG mode (AWG_m) excited by the geometrical ray $(Q \to A)$ incident on the edge A.

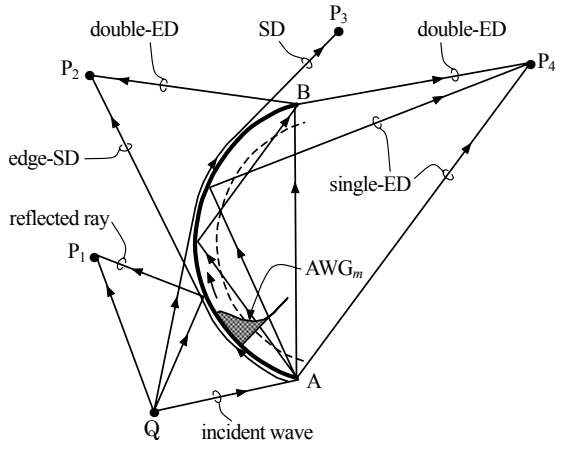

Fig.2 Single and double edge diffracted rays (single and double-ED), edge-surface diffracted rays (edge-SD) excited either by the edge A or both by the edges A and B. Also shown are geometrical rays (GO) including direct ray and reflected ray, and SD excited on the convex side by source Q.

radian frequency and the speed of light, respectively) i.e., $\omega a(s)/c >> 1$, and the source Q and the observation point P (R, ψ) are located sufficiently away from the curved surface.

When the cylindrical wave emanated from the source Q is incident on the edge A of the curved surface Ω, the edge diffracted ray (ED), the creeping wave (CW), and the lower order *m*th order adiabatic WG mode (AWG_m) [9], [10] are excited in the respective regions (see Fig.1). These waves excited at the edge A propagate toward the edge B direction and become new incident waves on the edge B (see Fig.1). Fig.2 shows geometrically the scattering phenomena when the cylindrical wave is incident on the convex side of a cylindrically curved open conducting surface Ω with two edges A and B.

The transient scattered field solution $y(R, \psi, t) \equiv (y(t))$ can be obtained from the inverse Fourier transform of the product of the FD scattered field $u_d(\omega, R, \psi) \equiv (u_d(\omega))$ and the frequency spectrum $S(\omega)$ of the source function $s(t)$ as follows

$$y(t) = \frac{1}{2\pi} \int_{-\infty}^{\infty} u_d(\omega) S(\omega) \exp(-i\omega t)\, d\omega. \qquad (1)$$

We will apply the Gaussian-type modulated pulse source $s(t)$ given by [2], [11], [12]

$$s(t) = \{U(t) - U(t - 2t_0)\} \cdot \exp\{-i\omega_0 (t - t_0) - (t - t_0)^2 / (4d^2)\} \qquad (2)$$

where $U(\bullet)$ is the unit step function and ω_0 is the central

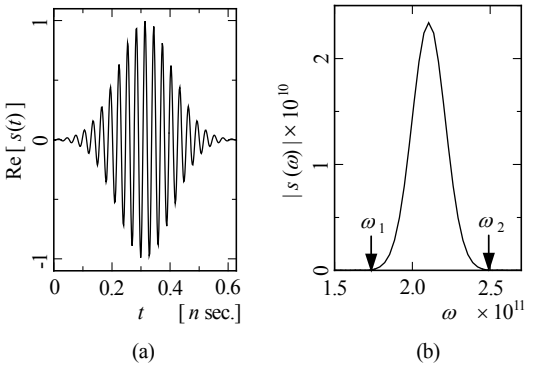

Fig.3 Gaussian-type modulated pulse source. (a) Real part of $s(t)$ in (2) with numerical parameters: $t_0 = 3.14 \times 10^{-10}$, $d = 6.60 \times 10^{-11}$, and $\omega_0 = 2.10 \times 10^{11}$. (b) Frequency spectrum $S(\omega)$ of the source function $s(t)$, and $\omega_1 \approx 1.76 \times 10^{11}$ and $\omega_2 \approx 2.45 \times 10^{11}$.

radian frequency modulating the pulse, and t_0 and d the constant parameters. The frequency spectrum $S(\omega)$ obtained by the Fourier transform of the source function $s(t)$ is given by

$$S(\omega) = 2d\sqrt{\pi} \exp\{i\omega t_0 - d^2(\omega - \omega_0)^2\} \operatorname{Re}[\operatorname{erf} \beta(\omega)] \qquad (3)$$

$$\beta(\omega) = t_0/(2d) - id(\omega - \omega_0) \qquad (3a)$$

where $\operatorname{Re}[\bullet]$ denotes the real part of $[\bullet]$. Fig.3 illustrates the source function $s(t)$ and its spectrum $S(\omega)$. The main portion of the frequency spectrum $S(\omega)$ is distributed in the HF domain approximately from $\omega = \omega_1$ to $\omega = \omega_2$, so that the integration interval in the inverse Fourier transform (1) can be changed from $(-\infty, \infty)$ to (ω_1, ω_2) (see Fig.3). Then, the FD scattered field $u_d(\omega)$ in (1) can be evaluated asymptotically under the HF assumption $\omega a(s)/c >> 1$. The FD-UAS $u_{d,asy}(\omega)$ for $u_d(\omega)$ can be represented as follows [8]

$$u_d(\omega) \sim u_{d,asy}(\omega) = u_{d,1}(\omega) + u_{d,2}(\omega) + u_{d,WG,m}(\omega) \qquad (4)$$

where $u_{d,1}(\omega)$ denotes the geometrical rays (GO) including the reflected ray and the ED, $u_{d,2}(\omega)$ the surface diffracted ray (SD) including the edge-SD, and $u_{d,WG,m}(\omega)$ the AWG_m radiation fields (see Fig.2).

After substituting the $u_{d,asy}(\omega)$ in (4) into $u_d(\omega)$ in (1), the integral $y(t)$ can be evaluated by applying the HF asymptotic analysis methods in **3**. While, substituting the FD-numerical solution $u_{d,\mathrm{MoM}}(\omega)$ obtained from the MoM into $u_d(\omega)$ in (1), one may obtain the numerical solution $y_{\mathrm{MoM}}(\mathrm{FFT})$ by applying the FFT code. The numerical solution $y_{\mathrm{MoM}}(\mathrm{FFT})$ thus obtained serves as the reference solution in **4**.

3. TIME –DOMAIN UNIFORM ASYMPTOTIC SOLUTION

3.1 Uniform Asymptotic Analysis by Saddle Point Technique

In this section, we will derive the TD-UAS for the GO and the SD. First, let's take the single-ED (see Fig.4), emanated from the edge A and arriving at the observation point P_4 after reflecting once on the concave boundary, as a simple and good example of $u_{d,1}(\omega)$. Then the $u_{d,1}(\omega)$ can be represented as follows [8]

$$u_{d,1}(\omega) = G(\mathrm{QA}) D_{\mathrm{A}}(\omega, \phi_{\mathrm{A}}, \phi_{\mathrm{A}}^{in}) G(\mathrm{AR}) \cdot \sqrt{dA(\mathrm{R})/dA(\mathrm{P}_4)}\, \exp(ik\mathrm{RP}_4 - i\pi/2) \tag{5}$$

where $G(x)$ denotes the 2-D Green's function

$$G(x) = \frac{i}{4}\sqrt{2c/\pi\omega x}\, \exp(i\omega x/c - i\pi/4) \tag{6}$$

and QA (AR) denotes the propagation distance of the ray traveling from the point Q (A) to the point A (R) (Henceforth, the distance between the point Q and A is indicated by QA). $D_{\mathrm{A}}(\omega, \phi_{\mathrm{A}}, \phi_{\mathrm{A}}^{in})$ is the edge diffraction coefficient for the observation angle ϕ_{A} and the incident angle ϕ_{A}^{in} and is given by

$$D_{\mathrm{A}}(\omega, \phi_{\mathrm{A}}, \phi_{\mathrm{A}}^{in}) = -\frac{F(X^i)}{\cos\frac{\phi_{\mathrm{A}} - \phi_{\mathrm{A}}^{in}}{2}} - \frac{F(X^r)}{\cos\frac{\phi_{\mathrm{A}} + \phi_{\mathrm{A}}^{in}}{2}} \tag{7}$$

$$F(X) = -2i\sqrt{X}\, \exp(-iX) \int_{\sqrt{X}}^{\infty} \exp(i\tau^2) d\tau \tag{7a}$$

$$X^i = 2\frac{\omega}{c}\frac{\mathrm{QA} \cdot \mathrm{AR}}{\mathrm{QA} + \mathrm{AR}} \cos^2\frac{\phi_{\mathrm{A}} - \phi_{\mathrm{A}}^{in}}{2} \tag{7b}$$

$$X^r = 2\frac{\omega}{c}\frac{\mathrm{AR} \cdot \rho^{\gamma}}{\mathrm{AR} + \rho^{\gamma}} \cos^2\frac{\phi_{\mathrm{A}} + \phi_{\mathrm{A}}^{in}}{2} \tag{7c}$$

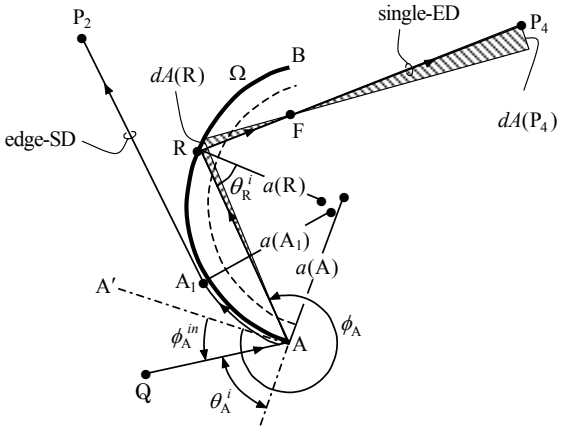

Fig.4 Single edge diffracted ray (single-ED) reflecting once on the concave boundary after the diffraction by the edge A and the edge surface diffracted ray (edge-SD).

$$\rho^{\gamma} = \frac{\mathrm{QA} \cdot a(\mathrm{A}) \cos\theta_{\mathrm{A}}^{in}}{2\mathrm{QA} + a(\mathrm{A}) \cos\theta_{\mathrm{A}}^{in}} \tag{7d}$$

In (5), $\sqrt{dA(\mathrm{R})/dA(\mathrm{P}_4)} = \sqrt{\mathrm{RF}/\mathrm{FP}_4}$ denotes the divergence coefficient, $dA(\mathrm{R})$ and $dA(\mathrm{P}_4)$ are the ray tube cross sections at R and P_4 (see Fig.4), respectively. $\mathrm{RP}_4 = (\mathrm{RF} + \mathrm{FP}_4)$ is the propagation distance from the reflection point R to P_4. $(-\pi/2)$ phase shift arises from the caustic F. RF is given as follows

$$\mathrm{RF} = \frac{\mathrm{AR} \cdot a(\mathrm{R}) \cos\theta_{\mathrm{R}}^{i}}{2\mathrm{AR} - a(\mathrm{R}) \cos\theta_{\mathrm{R}}^{i}} \tag{8}$$

where θ_{R}^{i} and $a(\mathrm{R})$ denote the incident angle and the radius of curvature at the point R, respectively.

The geometrical ray $u_{d,1}(\omega)$ in (5) can be expressed by

$$u_{d,1}(\omega) = A_1(\omega) \exp(i\omega L_1/c) \tag{9}$$

$$L_1 = \mathrm{Q} \to \mathrm{A} \to \mathrm{R} \to \mathrm{P}_4 \tag{9a}$$

where $A_1(\omega)$ is the slowly varying amplitude as the function of ω and L_1 denotes the propagation distance (see Fig.4) which is independent of ω.

Next, as an example of $u_{d,2}(\omega)$, we will consider the edge-SD propagating along the convex surface after the diffraction by the edge A (see Fig.4). This may be represented as [8]

$$u_{d,2}(\omega) = G(\mathrm{QA}) \sum_{\ell=1}^{\infty} \left\{ D_{\mathrm{A}}(\omega, \phi_{\ell}, \phi_{\mathrm{A}}^{in}) \frac{L_{\ell}(\mathrm{A})}{2} T_{\ell}(\mathrm{A}, \mathrm{A}_1) \cdot D_{\ell}(\mathrm{A}_1) \right\} G(\mathrm{A}_1\mathrm{P}_2) \tag{10}$$

$$L_{\ell}(\mathrm{A}) = (2\sigma_{\ell})^{-1/2} (\omega a(\mathrm{A})/2c)^{-1/6} \exp(i\pi/12) \tag{10a}$$

$$T_{\ell}(\mathrm{A}, \mathrm{A}_1) = \exp(i\omega\ell_1/(2c) - \Omega_{\ell}\ell_1), \quad \ell_1 = \int_{\mathrm{A}}^{\mathrm{A}_1} dt' \tag{10b}$$

$$\Omega_{\ell}\ell_1 = \sigma_{\ell} \exp(-i\pi/6) \int_{\mathrm{A}}^{\mathrm{A}_1} \frac{M(t')}{a(t')} dt' \tag{10c}$$

$$D_{\ell}(\mathrm{A}_1) = \sqrt{2}\left(\omega a(\mathrm{A}_1)/(2c)\right)^{1/6} \frac{\exp(-i\pi/12)}{\sqrt{\sigma_{\ell}}\, Ai(-\sigma_{\ell})} \tag{10d}$$

where $\phi_{\ell}(\nu_{\ell} = ka(\mathrm{A})\cos\phi_{\ell})$ denotes the eigen value of the ℓ th order CW satisfying the characteristic equation $H_{\nu_{\ell}}^{(1)\prime}(ka(\mathrm{A})) = 0$. The notations $L_{\ell}(\mathrm{A})$, $T_{\ell}(\mathrm{A}, \mathrm{A}_1)$, and $D_{\ell}(\mathrm{A}_1)$ are the launching coefficient from the edge A, the transmission coefficient from the edge A to the surface diffraction point A_1, and the surface diffraction coefficient at A_1, respectively (see Fig.4). The function $Ai(\bullet)$ is the Airy function [13]. $u_{d,2}(\omega)$ in (10) may be represented by the product of $A_2(\omega)$ and the phase term including the total propagation distance L_2 as follows:

$$u_{d,2}(\omega) = A_2(\omega)\exp(i\omega L_2/c) \tag{11}$$

$$L_2 = \mathrm{Q} \to \mathrm{A} \curvearrowright \mathrm{A}_1 \to \mathrm{P} \tag{11a}$$

The notation $\mathrm{A} \curvearrowright \mathrm{A}_1$ is used to indicate the CW propagation from A to A_1 along the arc of the curved surface Ω.

Substituting $u_{d,j}(\omega)$, $j = 1, 2$, in (9) or (11) and $S(\omega)$ in (3) into the inverse Fourier transform in (1) yields the following TD-integral representation

$$y_j(t) = \frac{d}{\sqrt{\pi}} s(t - L_j/c) I_j(\gamma), \quad j = 1, 2 \tag{12}$$

$$I_j(\gamma) = \frac{1}{2d^2}\int_{\omega'_1}^{\omega'_2} A_j(\omega'/(2d^2))\,\mathrm{Re}[erf\beta(\omega'/(2d^2))] \cdot \exp[-\gamma h_j(\omega')]\,d\omega' \tag{12a}$$

$$h_j(\omega') = \left[(\omega' - \omega'_0) + i(t - t_0 - L_j/c)\right]^2 \tag{12b}$$

$$\gamma = 1/(4d^2), \quad \omega'_0 = 2d^2\omega_0. \tag{12c}$$

In obtaining the above representations from (1), the transformation from ω to ω' via $\omega' = 2d^2\omega$ has been performed. Note that $\omega'_{1,2} = 2d^2\omega_{1,2}$.

For the large value of $\gamma\,(>>1)$, the integral $I_j(\gamma)$ in (12a) can be evaluated asymptotically by applying the saddle point technique [11], [12], [14]. The result is given by

$$I_j(\gamma) \sim \frac{\sqrt{\pi}}{d} A_j\left(\frac{\omega'_{j,s}}{2d^2}\right)\mathrm{Re}\left\{erf\beta\left[\frac{\omega'_{j,s}}{2d^2}\right]\right\} \tag{13}$$

where $\omega'_{j,s}$ is the saddle point :

$$\omega'_{j,s} = \omega'_0 - i(t - t_0 - L_j/c) \tag{13a}$$

in the complex ω'-plane determined from the saddle point equation $(\partial/\partial\omega')\cdot h_j(\omega') = 0$. Then substituting (13) into (12), the TD-UAS for the GO (j=1) and the SD (j=2) may be represented by

$$y_j(t) = A_j(\omega_{j,s})\,\mathrm{Re}[erf\beta(\omega_{j,s})]\,s(t - L_j/c) \tag{14}$$

$$\omega_{j,s} = \omega'_{j,s}/(2d^2) = \omega_0 - i(t - t_0 - L_j/c)/(2d^2). \tag{14a}$$

It is shown in (14) that the transient scattered field propagates with the phase velocity c and is observed after the total propagation time L_j/c.

3.2 Uniform Asymptotic Analysis by Fourier Transform Method

The solution $u_{d,WG,m}(\omega)$ in (4) for the mth order AWG_m radiation field from aperture plane at the edge B can be inferred from the result given in [8], [9], [11] and be represented as fofflows

$$u_{d,WG,m}(\omega) = U(\mathrm{P})\,u_{m,go}(\omega) + u_{m,d}(\omega) \tag{15}$$

$$u_{m,go}(\omega) = G(\mathrm{QA})D_{\mathrm{A}}(\omega, \phi_{\mathrm{A}}, \phi_{\mathrm{A}}^{in})\,G_{m,go}(\omega) = A_{m,go}(\omega)\exp(i\omega L_{m,go}(\omega)/c) \tag{15a}$$

$$u_{m,d}(\omega) = G(\mathrm{QA})D_{\mathrm{A}}(\omega, \phi_{\mathrm{A}}, \phi_{\mathrm{A}}^{in})\,G_{m,d}(\omega) = A_{m,d}(\omega)\exp(i\omega L_{m,d}(\omega)/c) \tag{15b}$$

$$G_{m,go}(\omega) = G_m^i(\mathrm{R})\Gamma_h\sqrt{\mathrm{RF}/\mathrm{FP}}\exp(ik\mathrm{RP} - i\pi/2) \tag{15c}$$

$$G_m^i(\mathrm{R}) = M_{eq,m}(\mathrm{T}_3)\,G(\mathrm{T}_3\mathrm{R}) \tag{15d}$$

$$M_{eq,m}(\mathrm{T}_3) = G_m^r(\overline{\mathrm{R}})\exp(i\omega d'/c - i3\pi/4),\ d' = \overline{\mathrm{R}}\mathrm{T}_3 \tag{15e}$$

$$G_m^r(\overline{\mathrm{R}}) = \frac{K_m}{\sqrt{M(\mathrm{A})M(\overline{\mathrm{R}})}}\frac{W_2(-\sigma_m)}{2}\exp\{i\omega\mathrm{T}_0 \curvearrowright \mathrm{T}_2/c\} \tag{15f}$$

$$K_m = i/\{4\sigma_m Ai(-\sigma_m)\}, \quad M(\mathrm{A}) = (\omega a(\mathrm{A})/c)^{1/3} \tag{15g}$$

$$G_m^d(\mathrm{P}) = u_m^i(\mathrm{B})\,D_{\mathrm{B}}(\omega, \phi_{\mathrm{B}}, \phi_{\mathrm{B}}^{in})\,G(\mathrm{BP}). \tag{15h}$$

Where $G(\mathrm{QA})$ and $D_{\mathrm{A}}(\omega, w_m, w_{in})$ are the incident GO (see (6)) and the edge diffraction coefficient (see (7)), respectively, and $G_{m,go}(\omega)$ denotes the GO converted from the incident modal ray $G_m^i(\mathrm{R})$ and arriving at the observation point P. Therefore, $u_{m,go}(\omega)$ in (15a) denotes the GO (single-ED), converted from AWG_m and arriving at the observation point P located in the illuminated region between $\mathrm{RB}_{\mathrm{WG}}$ and $\mathrm{SB}_{\mathrm{WG}}$, with the total propagation

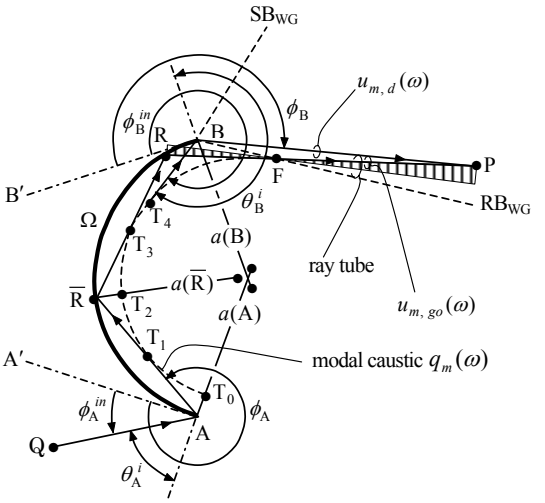

Fig.5 AWG_m radiation field from the aperture plane at the edge B. The solution observed at P can be represented by the combination of geometrical ray (single-ED) and the edge diffracted ray (double-ED).

distance $L_{m,go}(\omega)$ ($\approx$ Q $\rightarrow$ A $\rightarrow$ T_1 $\frown$ T_3 $\rightarrow$ R $\rightarrow$ P) While, $u_{m,d}(\omega)$ in (15b) denotes the edge diffracted ray (double-ED), excited by the incident modal ray G_m^i(B), with the total propagation distance $L_{m,d}(\omega)$ ($\approx$ Q $\rightarrow$ A $\rightarrow$ T_1 $\frown$ T_4 $\rightarrow$ B $\rightarrow$ P (see Fig.5). The notation $T_1 \frown T_{3,4}$ denotes the AWG$_m$ propagation from T_0 to $T_{3,4}$ along the arc of modal caustic defined by $q = q_m(\omega) = a(s) - \sigma_m (a(s)/2)^{1/3} \cdot (\omega/c)^{-2/3}$. Note that the total propagation distance $L_{m,j}(\omega)$, $j \equiv go$ or $j \equiv d$, changes as the function of ω.

U(P) in (15) is "one" when the observation point is located in the illuminated region and "zero" when it is in the shadow region. Substituting $u_{m,j}(\omega)$ in (15a) and (15b) and $S(\omega)$ in (3) into (1) yields the following TD-integral representation for the AWG$_m$ radiation field [11]

$$y_{m,j}(t) = \frac{1}{2\pi} \int_{-\infty}^{\infty} A_{m,j}(\omega) S(\omega) \exp[-i\omega\{t - L_{m,j}(\omega)/c\}]\, d\omega, \quad j \equiv go \text{ or } j \equiv d. \tag{16}$$

Since the total propagation distance $L_{m,j}(\omega)$ changes as the function of ω, it may be difficult to evaluate the integral $y_{m,j}(t)$ asymptotically by applying the saddle point technique. So, we will newly derive the uniform asymptotic solution, from the integral (16), by applying the Fourier transform method [11], [12].

The pulse source function $s(t)$ defined by (2) can be represented as follows

$$s(t) = \exp[-i\omega_0 (t - t_0)] p(t) \tag{17a}$$

$$p(t) = \exp[-(t - t_0)^2/(4d^2)]. \tag{17b}$$

Denoting the Fourier transform of $p(t)$ by $P(\omega)$, the frequency spectrum $S(\omega)$ in (3) can be represented as follows.

$$S(\omega) = \exp(i\omega_0 t_0) P(\omega - \omega_0) \tag{18}$$

$$P(\omega) = 2\sqrt{\pi} d \exp(i\omega t_0 - d^2\omega^2) \operatorname{Re}\{erf[\beta(\omega + \omega_0)]\} \tag{19}$$

Substituting (18) into (16) and evaluating the integral $y_{m,j}(t)$ in (16) by applying the Fourier transform method produce

$$y_{m,j}(t) = A_{m,j}(\omega_0) \exp[-i\omega_0 (t - t_0 - L_{m,j}(\omega_0)/c) - (t - t_0 - L_{m,j}(\omega_0)/v_{g,m,j})^2/(4d^2)] \tag{20}$$

$$v_{g,m,j} = c/(1 + \omega_0 L'_{m,j}(\omega_0)/L_{m,j}(\omega_0)). \tag{20a}$$

It is shown in (20) that the transient pulse wave for the AWG$_m$ radiation field propagates with the phase velocity c and the group velocity $v_{g,m,j}$ given by (20a).

4. Numerical Results And Discussions

In this section, we perform the numerical calculations necessary to assess the accuracy and the validity of the TD-UAS derived in **3**, and to interpret physically the phenomena of the transient scattered field. The pulse plane wave shown in Fig.3 is incident on the convex side of the cylindrically curved open surface Ω (see Fig.6) defined by

$$a(s) = 1/(a_0 - a_1 |s|), \quad |s| \le s_0 \tag{21}$$

where (a_0, a_1) are constant parameters and s_0 the arc length from the vertex point O to the edge A or B.

Fig.7(a) shows the real part of response waveform vs. time curves observed at $(R, \psi) = (0.8\,m, 100^\circ)$ (see Fig.1) when the pulse plane wave $s(t)$ is incident on the convex side of the curved surface Ω with the parameters $(a_0, a_1) = (10, 10)$ and s_0 = 0.096. The open circles (∘∘∘ : y_{MOM}(FFT)) are the numerical reference solution. The solid curve (—— : y_{asy}(FFT)) shows the numerical result obtained from the combination of the FD-UAS $u_{d,asy}(\omega)$ in (4) and the FFT code (see (1)). The solid curve agrees excellently with the reference solution in the whole region.

Although y_{MoM}(FFT) produces the numerical solution for the transient scattered field, it is difficult to separate each pulse individually from the total response waveform. While, y_{asy}(FFT) may be separated easily into each pulse, so that we shall use y_{asy}(FFT) as a new reference solution to assess the TD-UAS derived in **3** (see (14) and (20)). Fig.7(b) shows the pulses constituting the total response waveform in Fig.7(a). The closed circles (●●●) show the result of each TD-UAS (see Fig.6). Reflected ray (①), single-ED (②, ③), double -ED (④ ~ ⑦), edge-SD (⑧), and AWG$_1$ radiation fields (⑨ and ⑩) agree very well with the new reference solution shown by the solid curve (——).

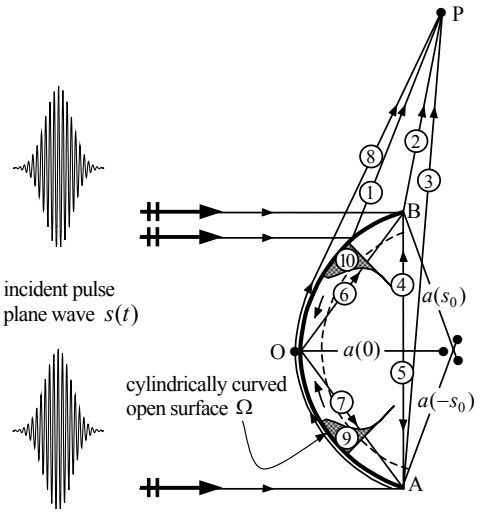

Fig.6 Scattered field observed at the point P. ① : reflected ray, ② and ③ : single-ED, ④ ~ ⑦ : double-ED, ⑧ : edge-SD, ⑨ and ⑩ : AWG$_1$ radiation fields.

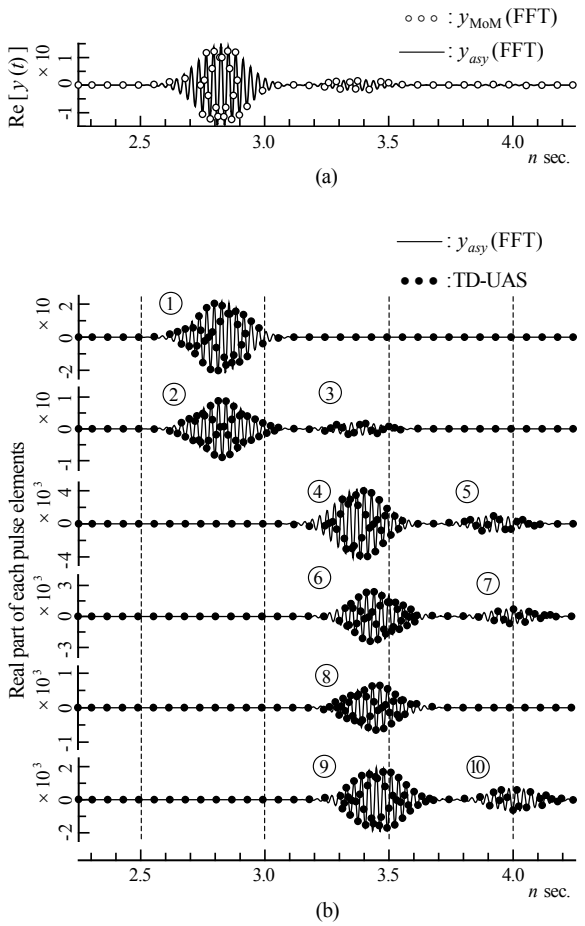

Fig.7 Total response waveform (Fig.7(a)) scattered by cylindrically curved open conducting surface and each pulse elements (Fig.7(b)). Numerical parameters: $(a_0, a_1) = (10, 10)$, $s_0 = 0.096$, and $(R, \psi) = (0.8m, 100°)$.

5. CONCLUSION

We have derived the time-domain uniform asymptotic solution (TD-UAS) for the transient scattered field by the cylindrically curved open conducting surface with a varying radius of curvature. The TD-UAS consists of the geometrical rays including the reflected rays and the edge diffracted rays, the surface diffracted rays, and the lowest order WG mode radiation fields, and the combination of these pulse waves. The accuracy and the validity of the TD-UAS proposed here have been confirmed by comparing with the numerical reference solutions obtained from (i) the combination of the method of moment and the FFT code and (ii) the combination of the frequency-domain uniform asymptotic solution and the FFT code. It has been shown that the TD-UAS is effective for physical interpretation of the scattered field since the pulses constituting the response waveform are observed separately.

REFERENCES

[1] L. B. Felsen, ed., *Transient Electromagnetic Fields*, Chaps.1-3, Springer-Verlag, New York, 1976.

[2] T. Ida, T. Ishihara, and K. Goto, "Frequency-domain and time-domain novel uniform asymptotic solutions for scattered fields by an impedance cylinder and a dielectric cylinder," *IEICE Trams. Electron.*, vol.E88-C, no.1, pp.2124-2135, Nov. 2005.

[3] J. B. Keller, "Diffraction by a convex cylinder," *IRE Trans. Antennas & Propag.*, vol.AP-4, pp.312-321, July 1956.

[4] J. B. Keller, "Geometrical theory of diffraction," *J. Opt. Soc. Am.*, vol.52, no.2, pp.116-130, Feb. 1962.

[5] G. L. James, ed., *Geometrical Theory of Diffraction for Electromagnetic Waves*, Peter Peregrinus Ltd., London, 3rd Edition, 1986.

[6] W. A. Johnson and R. W. Ziolkowski, "The scattering of an H-polarized plane wave from an axially slotted infinite cylinder: A dual series approach," *Radio Science*, vol.19, no.1, pp.275-291, 1984.

[7] R. F. Harrington, ed., *Field Computation by Moment Method*, R. E. Krieger Publishing Company, Malabar, Florida, Chaps.3 and 4, 1982.

[8] K. Goto and T. Ishihara, "High-frequency asymptotic analysis of scattered electromagnetic fields by conducting open curved surfaces with varying radius curvature"(in Japanese), *The Paper of Technical Meeting on EMT, IEE, Japan*, EMT-04-109, pp.25-31, Sept. 2004.

[9] T. Ishihara and K. Goto, "High-frequency analysis of electromagnetic fields on variable radius of concave conducting boundary"(in Japanese), *IEICE Trans.*, vol.J76-B-II, no.7, pp.605-614, July 1993.

[10] K. Goto, T. Ishihara, and L.B.Felsen, "High-frequency (whispering- gallery mode)-to-beam conversion on a perfectly conducting concave- convex boundary," *IEEE Trans. Antennas & Propag.*, vol.50, no.8, pp. 1109-1119, Aug. 2002.

[11] K. Goto and T. Ishihara, "Asymptotic analysis of transient whispering gallery mode radiation from a cylindrically curved conducting surface," *Proc. of 2005 IEEE AP-S International Symposium*, vol. 4B, pp.259-262, Washington, D.C., USA, July 2005.

[12] K. Goto, T. Ajiki, and T. Ishihara, "Asymptotic analysis of transient scattered field by a cylindrically curved conducting open surface," *Proc. of 2006 IEEE AP-S International Symposium*, vol.2, pp.1861-1864, Albuquerque, NM, UAS, July 2006.

[13] M.Abramowitz and I.A.Stegun, eds., *Handbook of Mathematical Functions*, Dover, New York, Chaps. 9 and 10, 1972.

[14] L. B. Felsen and N. Marcuvitz, eds., *Radiation and Scattering of Waves*, IEEE Press, New jersey, 1994.